

# Applications of the programmable two-dimensional optical fractional Fourier processor

José A. Rodrigo<sup>a \*</sup>, Tatiana Alieva<sup>b</sup>, Gabriel Cristóbal<sup>a</sup> and María L. Calvo<sup>b</sup>

<sup>a</sup> Instituto de Óptica (CSIC), Imaging and Vision Department, Serrano 121, Madrid 28006, Spain;

<sup>b</sup> Universidad Complutense de Madrid, Facultad de Ciencias Físicas, Ciudad Universitaria s/n, Madrid 28040, Spain.

## ABSTRACT

The fractional Fourier transform (FT) is a powerful tool with relevant applications in optical and digital information processing. Such applications demand a programmable and versatile optical system able to perform the fractional FT almost at real time. We have recently developed an optical setup satisfying these requirements. In contrast with other proposed setups, it offers the following advantages: the operation is achieved without additional scaling and/or phase factors and a minimal number of lenses, located at fixed position, are utilized.<sup>1</sup> In this work we present the main design features of the fractional FT processor and discuss its performance for some relevant applications.

**Keywords:** Fractional Fourier transform, Optical system design, Laser beam shaping.

## 1. INTRODUCTION

During the last decades, the fractional FT has demonstrated to play an important role in optics. The fractional FT is a generalization of the Fourier transform resulting very useful in many applications. It produces rotations of the Wigner distribution (WD), which describes the signal in phase space (time-frequency or space-frequency). In particular, it is a promising and versatile tool for beam characterization, phase retrieval, filtering, encryption, pattern recognition, etc.<sup>2,3</sup>

It was first introduced by Kober<sup>4</sup> in 1939 and then used in quantum mechanics by Namias<sup>5</sup> in 1980. This fractionalization of the FT was applied in optics almost two decades ago opening new perspectives in optical information processing.<sup>6-8</sup> Specifically, it was first studied by Mendlovic and Ozaktas when they analyzed gradient index (GRIN) fiber.<sup>6</sup> In the same year, Lohmann demonstrated that the fractional FT can be realized by using conventional lens-based systems.<sup>9</sup> A general treatment of optical systems performing the fractional FT was realized by Sahin et al. in 1998.<sup>8</sup> Other fractional transformations have been also studied in optics, see for example<sup>10</sup> and references therein.

The main applications of the fractional FT in optics require the fast modification of the fractional orders. Several optical systems performing the fractional FT have been proposed in the last years.<sup>11,12</sup> All these systems permit relatively easy to modify the fractional order but the resulting field amplitude is affected by an additional scaling that depends on the fractional order (also known as transformation angle), which in many cases is not desirable. Recently we have developed a fractional FT optical system that does not produce additional scaling and/or phase modulation of the transformed field.<sup>1</sup> This optical setup permits the change of the transformation parameters by means of power variation of the lenses, where the distance between them and input–output planes are fixed. These facts lead to a flexible optical setup able to perform the fractional FT by using a minimal number of lenses making easier its experimental implementation. Since each lens can be implemented by a spatial light modulator (SLM), to the advantages mentioned before one can also add the fast modification of the fractional orders reached almost at real time. Therefore this fractional FT optical setup can be considered as a promising tool for the above mentioned applications.

Our goal is to present the main setup features concerning to its experimental implementation. We also discuss its performance and feasibility considering some applications: beam characterization, optical mode conversion and phase retrieval.

---

\*E-mail: jose.a.rodrego@optica.csic.es.

## 2. OPTICAL SYSTEM DESIGN AND EXPERIMENTAL IMPLEMENTATION

The fractional FT setup is constructed by using three generalized lenses with fixed distance  $z$  between them, see Fig. 1, where the last lens and first one are identical ( $L_3 = L_1$ ). Each generalized lens  $L_1$  and  $L_2$  is an assembled set of two cylindrical lenses operating in orthogonal directions  $x$  and  $y$  axis, with variable lens power given as a function of the transformation angles  $\gamma_x$  and  $\gamma_y$ :

$$\begin{aligned} g_{x,y}^{(1)} &= z^{-1} (1 - \cot(\gamma_{x,y}/2) / 2), \\ g_{x,y}^{(2)} &= 2z^{-1} (1 - \sin \gamma_{x,y}), \end{aligned} \quad (1)$$

respectively. Notice that the phase modulation function associated with each generalized lens  $L_j$  ( $j = 1, 2$ ) takes the form:

$$\Psi_j(x, y) = \exp\left(-\frac{i\pi}{\lambda z} g_x^{(j)} x^2\right) \exp\left(-\frac{i\pi}{\lambda z} g_y^{(j)} y^2\right). \quad (2)$$

This optical configuration corresponds to the fractional FT operation defined as

$$\begin{aligned} F^{\gamma_x, \gamma_y}(\mathbf{r}_o) &= \frac{1/2\lambda z}{\sqrt{\sin \gamma_x \sin \gamma_y}} \iint f(x_i, y_i) \exp\left(i\pi \frac{(x_o^2 + x_i^2) \cos \gamma_x - 2x_i x_o}{2\lambda z \sin \gamma_x}\right) \\ &\times \exp\left(i\pi \frac{(y_o^2 + y_i^2) \cos \gamma_y - 2y_i y_o}{2\lambda z \sin \gamma_y}\right) dx_i dy_i, \end{aligned} \quad (3)$$

where  $\lambda$  is the wavelength,  $\mathbf{r}_{i,o} = (x_{i,o}, y_{i,o})$  are the input and output spatial coordinates while  $f(\mathbf{r}_i)$  is a complex amplitude of monochromatic input field.<sup>1</sup> Notice that  $s^2 = 2\lambda z$  is a coordinate normalization. The fractional FT setup allows the modification of the transformation angles inside a  $\pi$ -interval:  $\gamma_{x,y} \in [\pi/2, 3\pi/2]$ , see Fig. 2. It is sufficient for the most of applications, however since the relation  $F^{\gamma_x+\pi, \gamma_y+\pi}(\mathbf{r}_i, \mathbf{r}_o) = F^{\gamma_x, \gamma_y}(\mathbf{r}_i, -\mathbf{r}_o)$  holds then the interval  $\gamma_{x,y} \in (0, 2\pi)$  can be also reached.

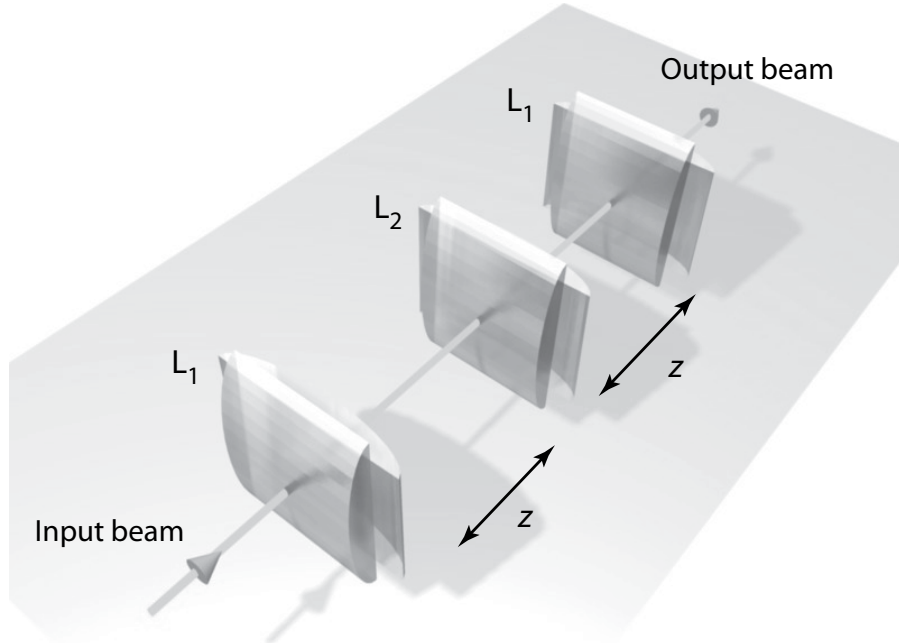


Fig. 1. Fractional FT optical setup. Each generalized lens is an assembled set of two cylindrical lenses crossed at angle  $\pi/2$ . Their lens power are functions of the transformation angles, as it is described by Eq. (1). The distance  $z$  between consecutive lenses is fixed. Notice that the input and output plane of the setup coincide with the plane containing first and last lenses.

For angles  $\gamma_x = \gamma_y = 0$  the fractional FT reduces to identity transformation whereas for  $\gamma_x = 0$  and  $\gamma_y = \pi$  image reflection is obtained. Meanwhile for  $\gamma_x = \gamma_y = \pi/2$  the Fourier transform holds. The case  $\gamma_x = \gamma_y = \gamma$  and  $\gamma_x = -\gamma_y = \gamma$  correspond to the symmetric and antisymmetric fractional FT up to a constant phase shift, respectively. It is usual to define the transformation angle as  $\gamma = q\pi/2$ , where  $q$  is the fractional order. For instance, order  $q = 4$  leads to the self-imaging case meanwhile  $q = -1$  corresponds to the inverse Fourier transform. We also mention that the fractional FT is an additive operation with respect the transformation angles. The fractional FT kernel is given as a product of plane and elliptic waves. Properties and applications of the fractional FT operation are discussed in detail for example in Ref. 2 .

Most of applications such as beam characterization, phase retrieval, chirp detection, etc., demand only the acquisition of the fractional FT squared moduli  $|F^{\gamma_x, \gamma_y}(\mathbf{r}_o)|^2$  (power spectra) for various angles, associated with intensity distributions. These intensity distributions are projections of the Wigner distribution  $W_f(\mathbf{r}, \mathbf{p})$ , where  $\mathbf{p} = (p_x, p_y)$  corresponds to the spatial frequencies. In other words it takes the form:

$$|F^{\gamma_x, \gamma_y}(\mathbf{r})|^2 = \int W_f(x \cos \gamma_x - sp_x \sin \gamma_x, y \cos \gamma_y - sp_y \sin \gamma_y, s^{-1}x \sin \gamma_x + p_x \cos \gamma_x, s^{-1}y \sin \gamma_y + p_y \cos \gamma_y) dp_x dp_y, \quad (4)$$

see for example<sup>13</sup> and references therein. Therefore the implementation of the third generalized lens ( $L_3 = L_1$ ) is not required in such case.

The fast modification of the transformation angles, directly related to the generalized lens powers [Eq. (1)], can be achieved by using a SLM for the lens implementation. In conclusion, at least two SLMs have to be used simultaneously. In our case we use two reflection SLMs operating in phase-only modulation with 256 gray levels and pixel size of 19  $\mu\text{m}$  (Holoeye LCR-2500). The corresponding setup is depicted in Fig. 3, where two cube beam splitter are set for beam redirecting.

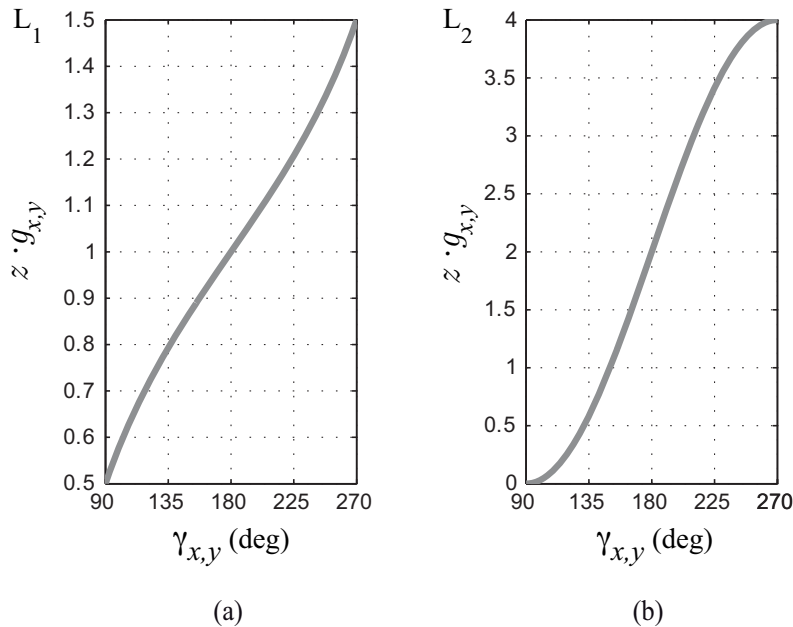


Fig. 2. Normalized lens power variation  $z g_{x,y}$  depicted as a function of the transformation angles  $\gamma_{x,y}$  [see Eq. (1)] for the first (a) and second (b) generalized lens.

This programmable optical setup performs the fractional FT operation almost at real time and its result can be also stored as a video by using a CCD camera. Indeed, this fact has been demonstrated achieving a speed operation of 3  $\text{deg}\cdot\text{s}^{-1}$ , which is limited by the SLM refresh rate.<sup>1</sup> Alignment between the SLMs (lenses  $L_1$  and  $L_2$ ) can be reached digitally as well. It makes easier its implementation and reduces cost because a high-accuracy positioning X-Y stage for each SLM is not required.

In order to reduce the noise arising from the SLM structure several relevant facts have to be considered. First we mention that both SLM are slightly tilted (2-3 degrees) in such way that first diffraction and zeroth orders do not overlap. Notice that the zeroth order carries unmodulated light which is mainly caused by the limited fill factor of the SLM. Meanwhile the nonlinear response of the SLM and the deviation from flatness of its reflective surface lead to distortions in phase modulation that could be reduced applying wavefront correction techniques as it is discussed in.<sup>14</sup> Besides we mention that the input beam, modulated by the displayed phase pattern, is diffracted into the first diffraction order with an efficiency close to 45%. Since two cube beam splitters (50:50 splitting) are utilized, see Fig. 3, the power ratio between input and output beams is significantly reduced as well. In spite of these issues, mainly caused by the SLM, the transformation is achieved without considerable quality reduction as it will be demonstrated in the next Section.

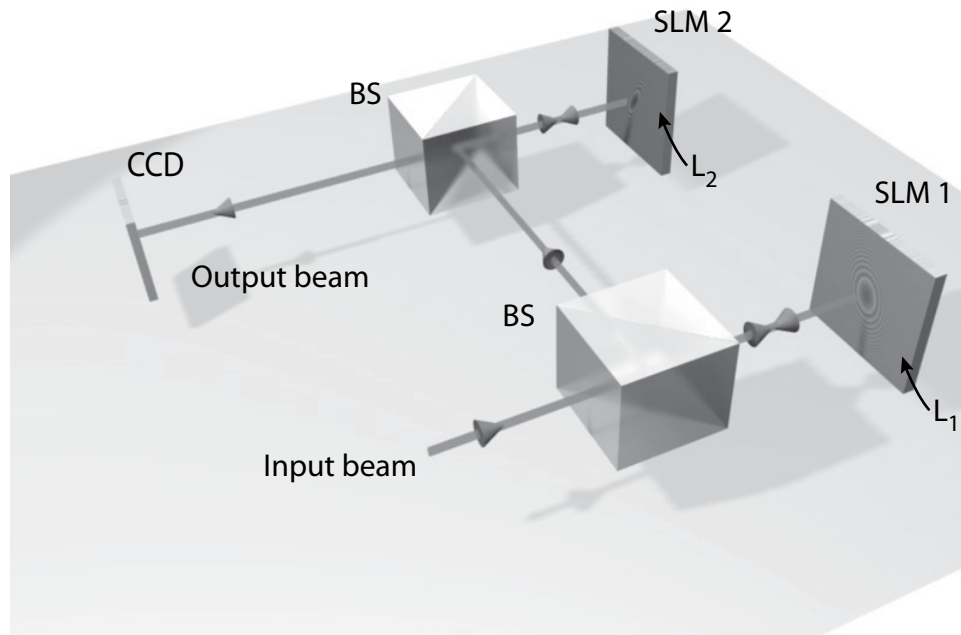


Fig. 3. Scheme corresponding to the proposed fractional FT setup. Phase-only spatial light modulator SLM1 and SLM2 implement generalized lens  $L_1$  and  $L_2$ , respectively. Optical path between lenses and CCD camera is fixed at  $z = 50$  cm. Both SLMs share the same DVI interface: display data channel red and green.

The input signal can be generated for example by modulating a collimated laser beam. In general any complex 2D input signal  $f(\mathbf{r}_i)$  can be implemented into a SLM by means of a phase-only hologram, which in our case can be addressed together with the generalized lens  $L_1$ . In such kind of hologram,  $H(x_i, y_i)$ , the phase distribution  $\arg[f(x_i, y_i)]$  is spatially modulated by the amplitude distribution  $|f(x_i, y_i)|$  associated to the input signal<sup>15,16</sup> as following:

$$H(x_i, y_i) = \exp \{ i |f(x_i, y_i)| (\arg[f(x_i, y_i)] + 2\pi x_i / \Lambda) \}, \quad (5)$$

where  $\Lambda$  is the grating period whereas the phase and amplitude range are  $[-\pi, \pi]$  and  $0 < |f(x_i, y_i)| < 1$  respectively. We underline that the input signal  $f(\mathbf{r}_i)$  is fully recovered into the first diffraction order only under certain conditions which are discussed in detail in.<sup>15</sup>

Alternatively, the amplitude distribution can be addressed into a transmissive SLM operating in amplitude-only modulation and then projected (by using a 4-f lens system or telescope) into a phase-only SLM, where its corresponding phase distribution is displayed.<sup>1</sup> In our case we have chosen this approach because it permits an accurate input signal generation. It is also highly recommended for setup testing. Figure 4 shows the corresponding experimental setup.

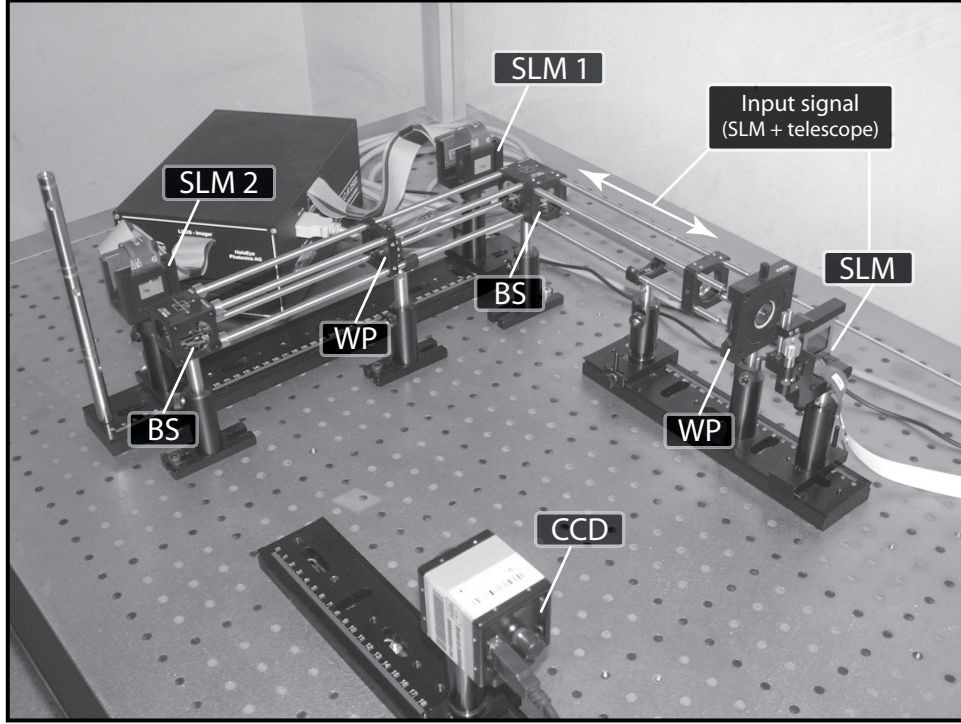


Fig. 4. Programmable fractional FT processor. In this case the input signal is generated as following: its amplitude distribution is addressed onto SLM and then projected (by using a telescope) into SLM1 which displays its phase distribution together with the generalized lens  $L_1$ . A  $\lambda/2$  wave-plate (WP) is set in order to achieve phase-only modulation.

### 3. EXAMPLES AND MAIN APPLICATIONS

Since the transformation of Hermite–Gaussian (HG) and Laguerre–Gaussian (LG) beams under the fractional FT is well-established, its study serves as a calibration approach of the proposed setup. Therefore in order to test the experimental setup we can choose as an input signal the Hermite–Gaussian

$$HG_{m,n}(\mathbf{r}; w) = 2^{1/2} \frac{H_m(\sqrt{2\pi} \frac{x}{w}) H_n(\sqrt{2\pi} \frac{y}{w})}{\sqrt{2^m m! w} \sqrt{2^n n! w}} \exp\left(-\frac{\pi}{w^2} r^2\right), \quad (6)$$

or Laguerre–Gaussian

$$LG_{p,l}^{\pm}(\mathbf{r}; w) = w^{-1} \left(\frac{p!}{(p+l)!}\right)^{1/2} \left(\sqrt{2\pi} \frac{x \pm iy}{w}\right)^l L_p^l\left(\frac{2\pi}{w^2} r^2\right) \exp\left(-\frac{\pi}{w^2} r^2\right) \quad (7)$$

beams, where:  $r^2 = x^2 + y^2$ ,  $H_m$  is the Hermite polynomial,  $w$  is the beam waist, and  $L_p^l$  is the Laguerre polynomial with radial index  $p$  and azimuthal index  $l$ . For instance a LG mode under antisymmetric fractional FT at angle  $\gamma = (2k+1)\pi/4$  (with  $k$  integer) is transformed into a HG mode and vice versa, where  $p = \min(m, n)$  and  $l = |m - n|$ . For the rest of transformation angles an intermediate HG–LG mode is obtained. As an example, in Fig. 5 we present the experimental results corresponding to this transformation at angles  $\gamma = 225^\circ$ ,  $248^\circ$  and  $259^\circ$  with input signal  $LG_{4,1}^+$ . As it is demonstrated in Fig. 5, the experimental results are in good agreement with the theoretical predictions. We underline that the wavefront distortion mainly arising from SLM structure does not produce considerable quality reduction.

Other important issue to be considered concerns to the beam collimation quality as well as telescope performance, used for input signal generation. For instance if the telescope and/or beam collimation are not properly set then an additional quadratic phase modulation is obtained. This additional wavefront distortion has to be minimized in order to achieve fine-tuning of the fractional FT operation.

We remind that the  $LG_{p,l}^{\pm}$  mode is a vortex beam carrying an Orbital Angular Momentum (OAM):  $l\hbar$  per photon. Meanwhile an intermediate HG–LG modes carries fractional OAM:  $l\hbar \sin 2\gamma$ , see.<sup>17</sup> In contrast to the LG beams, which are widely used in different areas, the application of HG–LG one is still under development. Therefore the proposed fractional FT setup results useful for applications involving mode conversion as well. For example, the HG–LG modes could be also useful in quantum computing<sup>18</sup> and optical trapping.

The fractional FT operation can be used for beam characterization based on measurements of the WD moments. Notice that second-order moments of the WD are the basis of an International Organization for Standardization standard, see.<sup>19</sup> It permits to perform the phase-space tomography required for the reconstruction of the WD and therefore for phase or mutual intensity of coherence (or partially coherence) field.<sup>13</sup> Therefore the proposed setup can be considered as a promising tool for beam characterization. In addition, this optical design may be suitable for other applications where the fractional FT operation has demonstrated its feasibility: filtering, image denoising,<sup>20</sup> correlation and pattern recognition,<sup>21–23</sup> among others. Nevertheless it requires at least a cascade of two fractional FT setups and therefore four SLMs (note that several lenses can be multiplexed into a single SLM).

Here we consider as an example the phase retrieval of two-dimensional coherent signals demonstrating experimentally its performance. There exist different phase retrieval procedures involving interferometric techniques or iterative algorithms based on measurements of the intensity distribution. In particular, we consider an iterative phase retrieval approach based on the well-known Gerchberg-Saxton algorithm.<sup>24</sup> Notice that this algorithm is often based on the Fourier power spectrum measurement. To retrieve the input phase distribution, up to constant, we apply the approach reported in<sup>25</sup> that requires several measurements of intensity distributions associated to the power spectra of the fractional FT. These images play the role of constraint planes. As it is demonstrated in<sup>25</sup> the algorithm convergence speeds up with respect to common approaches based on the FT, in which one intensity distribution is only utilized as an output constraint plane. In our case we consider the antisymmetric fractional FT operation instead of the symmetric one studied in the latter work. The power spectra obtained for this transformation at angles  $\gamma = 225^\circ$ ,  $248^\circ$  and  $259^\circ$  (constraint output planes) are displayed in Fig. 5(b)-(d), where the input signal is a  $LG_{4,1}^+$  mode Fig. 5(a).

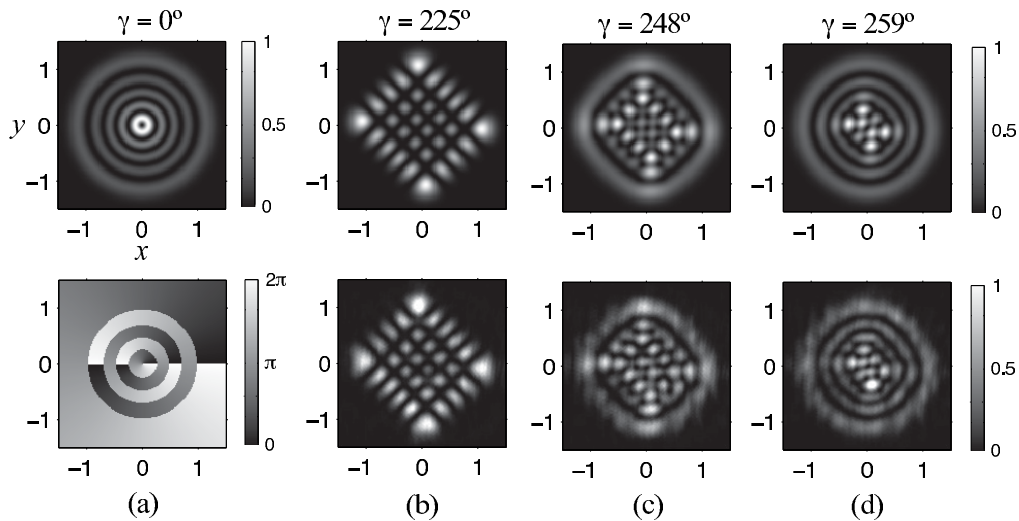


Fig. 5. (a) Input signal,  $LG_{4,1}^+$  mode. (b)-(d) Numerical and experimental results (first and second row respectively) corresponding to power spectra of antisymmetric fractional FT at angles  $\gamma = 225^\circ$ ,  $248^\circ$  and  $259^\circ$ . The beam waist was set at  $w = 0.73$  mm and wavelength  $\lambda = 532$  nm. Notice that for  $\gamma = 225^\circ$  the LG input mode is transformed into a HG one rotated at  $45^\circ$ . The experimental results were registered by using a CCD camera with pixel size of  $4.6 \mu\text{m}$ . Units in  $x$  and  $y$  axis are given in mm.

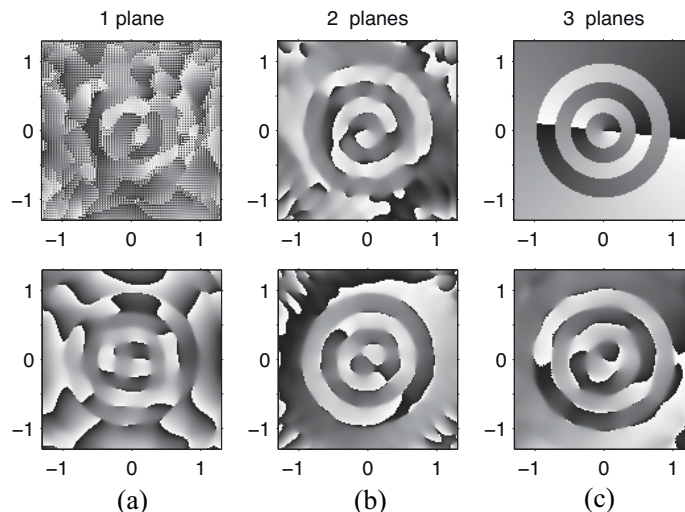


Fig. 6. Retrieved phase distribution associated to the  $LG_{4,1}^+$  mode corresponding to numerical (after 30 iterations) and experimental results (after 300 iterations), first and second row respectively. The phase distribution is fully retrieved after 30 iterations with 3 constrain planes corresponding to  $\gamma = 225^\circ, 248^\circ$  and  $259^\circ$ , see Fig. 5(b)-(d). Meanwhile the convergence for the experimental retrieved phase is reached with root mean squared error of 40%, caused by wavefront distortions.

After enough number of iterations the convergence occurs, which is reduced by increasing the number of constraint planes or images used. This fact is demonstrated in Fig. 6 by using numerical and experimental results, first and second row respectively. Notice that the number of iterations remains fixed in each case. As we have previously discussed, the experimental results displayed in Fig. 5(b)-(d) also includes the wavefront distortion which is mainly caused by the SLM structure due to its fabrication.<sup>14</sup> Therefore this phase retrieval technique is also suitable for the fractional FT setup testing. Moreover the corresponding corrective phase pattern can be calculated from the retrieved phase distribution Fig. 6(c), and then addressed into the SLM in order to compensate such distortion. Nevertheless it requires a further analysis which exceeds the scope of this work.

#### 4. CONCLUSIONS

We have presented an optical system able to perform automatically the two-dimensional fractional FT operation almost at real time. In contrast with other proposed setups, the transformation is achieved without additional scaling and/or phase factors. By using SLMs for lens implementation as well as for input signal generation, we demonstrate experimentally its performance and feasibility for applications such as mode conversion and phase retrieval. The experimental results are in good agreement with theoretical predictions. Other relevant applications for optical information processing based on the proposed setup are still under development.

#### ACKNOWLEDGMENTS

The financial support of the Spanish Ministry of Science and Innovation under projects TEC2005-02180, TEC2008-04105, TEC2007-67025/TCM, TEC2007-30709E and Santander-Complutense project PR-34/07-15914 are acknowledged. José A. Rodrigo also thanks a “Juan de la Cierva” grant.

#### REFERENCES

1. Rodrigo, J. A., Alieva, T., and Calvo, M. L., “Programmable two-dimensional optical fractional Fourier processor,” *Opt. Express* **17**(7), 4976–4983 (2009).
2. Ozaktas, H. M., Zalevsky, Z., and Kutay, M. A., [*The Fractional Fourier Transform with Applications in Optics and Signal Processing*], John Wiley&Sons, NY, USA (2001).

3. McAlister, D. F., Beck, M., Clarke, L., Mayer, A., and Raymer, M. G., "Optical phase retrieval by phase-space tomography and fractional-order Fourier transforms," *Opt. Lett.* **20**(10), 1181–1183 (1995).
4. Kober, H., "Wurzeln aus der Hankel-, Fourier- und aus anderen stetigen Transformationen," *Quart. J. Math. Oxford.* **10**, 45–59 (1939).
5. Namias, V., "The fractional order Fourier transform and its applications to quantum mechanics," *Journal of the Institute of Mathematics and Its Applications* **25**, 241–265 (1980).
6. Mendlovic, D. and Ozaktas, H. M., "Fractional Fourier transform and their optical implementation," *J. Opt. Soc. Am. A* **10**, 1875–1881 (1993).
7. Lohmann, A. W., "Image rotation, Wigner rotation, and the fractional Fourier transform," *J. Opt. Soc. Am. A* **10**(10), 2181 (1993).
8. Sahin, A., Ozaktas, H. M., and Mendlovic, D., "Optical implementations of two-dimensional fractional Fourier transforms and linear canonical transforms with arbitrary parameters," *Appl. Opt.* **37**(11), 2130–2141 (1998).
9. Lohmann, A. W., "Image rotation, Wigner rotation, and the fractional order Fourier transform," *J. Opt. Soc. Am. A* **10**, 2181–2186 (1993).
10. Alieva, T., Bastiaans, M., and Calvo, M. L., "Fractional transforms in optical information processing," *EURASIP J. Appl. Signal Process* **2005**, 1498–1519 (2005).
11. Malyutin, A. A., "Tunable Fourier transformer of the fractional order," *Quantum Electron.* **36**, 79–83 (2006).
12. Moreno, I., Davis, J. A., and Crabtree, K., "Fractional Fourier transform optical system with programmable diffractive lenses," *Appl. Opt.* **42**, 6544–6548 (2003).
13. Cámara, A., Alieva, T., Rodrigo, J. A., and Calvo, M. L., "Phase space tomography reconstruction of the Wigner distribution for optical beams separable in cartesian coordinates," *J. Opt. Soc. Am. A* **26**(6), 1301–1306 (2009).
14. Jesacher, A., Schwaighofer, A., Fürhapter, S., Maurer, C., Bernet, S., and Ritsch-Marte, M., "Wavefront correction of spatial light modulators using an optical vortex image," *Opt. Express* **15**(9), 5801–5808 (2007).
15. Davis, J. A., Cottrell, D. M., Campos, J., Yzuel, M. J., and Moreno, I., "Encoding amplitude information onto phase-only filters," *Appl. Opt.* **38**(23), 5004–5013 (1999).
16. Bentley, J. B., Davis, J. A., Bandres, M. A., and Gutiérrez-Vega, J. C., "Generation of helical incoherent Gaussian beams with a liquid-crystal display," *Opt. Lett.* **31**(5), 649–651 (2006).
17. Alieva, T. and Bastiaans, M. J., "Orthonormal mode sets for the two-dimensional fractional Fourier transformation," *Opt. Lett.* **32**(10), 1226–1228 (2007).
18. Mair, A., Vaziri, A., Weihs, G., and Zeilinger, A., "Entanglement of the orbital angular momentum states of photons," *Nature* **412**, 313–316 (2001).
19. "Lasers and laser-related equipment—test methods for laser beam parameters—beam widths, divergence angle and beam propagation factor, ISO Doc. 11146: 1999. International Organization for Standardization, Geneva, Switzerland, 1999."
20. Ozaktas, H. M., Barshan, B., Mendlovic, D., and Onural, L., "Convolution, filtering, and multiplexing in fractional Fourier domains and their relation to chirp and wavelet transforms," *J. Opt. Soc. Am. A* **11**(2), 547 (1994).
21. Barshan, B. and Ayrulu, B., "Fractional Fourier transform pre-processing for neural networks and its application to object recognition," *Neural Networks* **15**, 131–140 (2002).
22. Lohmann, A. W., Zalevsky, Z., and Mendlovic, D., "Synthesis of pattern recognition filters for fractional Fourier processing," *Opt. Commun.* **128**, 199–204 (1996).
23. Garcia, J., Mendlovic, D., Zalevsky, Z., and Lohmann, A., "Space-variant simultaneous detection of several objects by the use of multiple anamorphic fractional-Fourier-transform filters," *Appl. Opt.* **35**(20), 3945 (1996).
24. Gerchberg, R. W. and Saxton, W. O., "A practical algorithm for the determination of phase from image and diffraction plane pictures," *Optik* **35**, 237–246 (1972).
25. Zalevsky, Z., Mendlovic, D., and Dorsch, R. G., "Gerchberg-Saxton algorithm applied in the fractional Fourier or the Fresnel domain," *Opt. Lett.* **21**(12), 842 (1996).